

ENERGY STABILITY AND ERROR ESTIMATES OF A MAXIMUM BOUND PRINCIPLE PRESERVING SCHEME FOR THE DYNAMIC GINZBURG-LANDAU EQUATIONS OF SUPERCONDUCTIVITY

LIMIN MA AND ZHONGHUA QIAO

ABSTRACT. The paper proposes a decoupled numerical scheme of the time-dependent Ginzburg-Landau equations under temporal gauge. For the order parameter and the magnetic potential, the discrete scheme adopts the second type Nedélec element and the linear element for spatial discretization, respectively, and a fully linearized backward Euler method and the first order exponential time differencing method for time discretization, respectively. The maximum bound principle of the order parameter and the energy dissipation law in the discrete sense are proved for this finite element-based scheme. This allows the application of the adaptive time stepping method which can significantly speed up long-time simulations compared to existing numerical schemes, especially for superconductors with complicated shapes. The error estimate is rigorously established in the fully discrete sense. Numerical examples verify the theoretical results of the proposed scheme and demonstrate the vortex motions of superconductors in an external magnetic field.

Keywords. Ginzburg–Landau equations, energy stability, maximum bound principle, error estimate, superconductivity, exponential time differencing method

1. INTRODUCTION

In this paper, we consider the transient behavior and vortex motions of superconductors in an external magnetic field \mathbf{H} which is described by the time-dependent Ginzburg-Landau (TDGL) equations [17]. This TDGL model was first established in [18] with some detailed description in [2, 8, 31]. The non-dimensional form of the TDGL equations solves (\mathbf{A}, ψ) satisfying

$$(1) \quad \begin{cases} (\partial_t + i\kappa\phi)\psi + \left(\frac{i}{\kappa}\nabla + \mathbf{A}\right)^2 \psi + (|\psi|^2 - 1)\psi = 0 & \text{in } \Omega \times (0, T], \\ \sigma(\nabla\phi + \partial_t\mathbf{A}) + \nabla \times (\nabla \times \mathbf{A}) + \operatorname{Re} \left[\psi^* \left(\frac{i}{\kappa}\nabla + \mathbf{A} \right) \psi \right] = \nabla \times \mathbf{H} & \text{in } \Omega \times (0, T], \end{cases}$$

with the boundary and initial conditions

$$(2) \quad \begin{cases} (\nabla \times \mathbf{A}) \times \mathbf{n} = \mathbf{H} \times \mathbf{n}, & \left(\frac{i}{\kappa}\nabla + \mathbf{A}\right)\psi \cdot \mathbf{n} = 0 & \text{on } \partial\Omega, \\ \psi(x, 0) = \psi^0(x), & \mathbf{A}(x, 0) = \mathbf{A}^0(x) & \text{on } \Omega, \end{cases}$$

where Ω is a bounded domain in $\mathbb{R}^d (d = 2, 3)$, \mathbf{n} is the unit outer normal vector, the magnetic potential \mathbf{A} is a real vector-valued function and the order parameter ψ is a complex scalar-valued function. Physically speaking, the magnitude of the order parameter $|\psi|$ represents the superconducting density, where $|\psi| = 0$ stands for normal state, $|\psi| = 1$ for superconducting state, and $0 < |\psi| < 1$ for a mixed state. It is proved in [4] that the order parameter in the TDGL equations (1) satisfies a maximum bound principle (MBP) in the sense that the magnitude of the order parameter is bounded by 1, i.e.

$$(3) \quad \|\psi(\cdot, t)\|_\infty \leq 1, \quad \forall t > 0$$

if the initial condition $\|\psi^0\|_\infty \leq 1$ and $\mathbf{A}^0 \in H^1(\Omega)$ with $\mathbf{A}^0 \cdot \mathbf{n}|_{\partial\Omega} = 0$. An energy dissipation law holds for any solution (\mathbf{A}, ψ) of the TDGL equations (1), which is

$$(4) \quad \frac{d}{dt}G(\mathbf{A}, \psi) \leq -4\pi(\mathbf{M}, \partial_t \mathbf{H}),$$

where the magnetization $\mathbf{M} = \frac{1}{4\pi}(\nabla \times \mathbf{A} - \mathbf{H})$ and the Gibbs energy functional

$$(5) \quad G(\mathbf{A}, \psi) = \frac{1}{2} \left\| \left(\frac{i}{\kappa} \nabla + \mathbf{A} \right) \psi \right\|_0^2 + \frac{1}{2} \|\nabla \times \mathbf{A} - \mathbf{H}\|_0^2 + \frac{1}{4} \|\psi\|_0^2 - 1\|_0^2.$$

Particularly, if the applied magnetic field \mathbf{H} is stationary, the Gibbs energy of a solution of (1) decreases in time. The solution of the TDGL equations (1) is not unique. A family of theoretically equivalent solutions of the TDGL equations (1) under a gauge transformation shares the same $|\psi|$ and magnetic induction field $\nabla \times \mathbf{A}$, which are of physical interest.

There are many works on the numerical schemes of the TDGL equations (1) under different gauges, especially the temporal gauge $\phi = 0$ and the Lorentz gauge $\phi = -\nabla \cdot \mathbf{A}$. On uniform rectangular meshes, a gauge-invariant backward Euler scheme and a stabilized semi-implicit Euler gauge-invariant scheme were proposed in [7] and [12], respectively. Both schemes preserve the discrete MBP and guarantee the boundedness of the energy in the sense that the energy is bounded by a multiple of the initial energy with the factor depending on the terminal time.

For the TDGL equations under the Lorentz gauge, the existing numerical schemes using finite element methods for spatial discretization employ an additional boundary condition, which is indispensable to guarantee the wellposedness of the discrete problems. Mixed element methods are widely used in solving the TDGL equations under the Lorentz gauge. A semi-implicit mixed element scheme was proposed in [3] with optimal convergence result. Two fully discrete schemes by mixed element methods were proposed in [14, 15] by treating $\nabla \times \mathbf{A}$ as an auxiliary variable, and a fully discrete mixed element scheme was proposed in [11] by treating $\nabla \times \mathbf{A}$ and $\nabla \cdot \mathbf{A}$ as two auxiliary variables. A fully discrete scheme with a mixed element method by using the Hodge decomposition was proposed in [23] with an optimal convergence analysis in [25]. The boundedness of energy was analyzed in [25] concerning a modified energy with an extra term $\frac{1}{2}\|\psi\|_0^2$ in the Gibbs energy (4). A new mixed element scheme on a general polygonal domain by using the Hodge decomposition was proposed in [22] with an optimal convergence analysis result. A linearized Crank–Nicolson Galerkin finite element method was proposed in [13] with an optimal second-order convergence analysis with respect to the time discretization. A linearized backward Euler Galerkin-mixed finite element method was proposed in [16] with optimal convergence analysis. Note that the energy stability results of numerical schemes for the TDGL equations under the Lorentz gauge are very limited, because the TDGL equations under this particular gauge are not derived from the energy view and cannot be viewed as a gradient flow of the Gibbs energy. The bounded energy of discrete schemes was usually analyzed by using the Gronwall inequality which makes the bound depend on the terminal time and might be incredibly large in long-time simulations.

The TDGL equations (7) under temporal gauge can be viewed as an L^2 -gradient flow with respect to $G(\mathbf{A}, \psi)$ and

$$(6) \quad \frac{d}{dt}G(\mathbf{A}, \psi) + \|\partial_t \mathbf{A}\|_0^2 + \|\partial_t \psi\|_0^2 = -4\pi(\mathbf{M}, \partial_t \mathbf{H}),$$

which benefits the energy stability analysis of numerical schemes under this particular gauge. A nonlinear finite element scheme with an extra perturbed term was proposed in [6] under an additional boundary condition besides (2). The scheme in [6] admits the discrete energy dissipation law under a strict constraint on the time step. Two linearized Crank–Nicolson–Galerkin with a similar perturbed term were proposed in [26, 27] under the aforementioned additional boundary condition and (2). In [27], a modified energy of the proposed scheme was proved to be bounded, and the magnitude of the discrete order parameter was bounded above under the assumption $\tau \lesssim h^{\frac{11}{12}}$ in two dimensions and $\tau \lesssim h^2$ in three dimensions, where the bound tends to large when the perturbation parameter tends to zero. Recently, a nonlinear finite element scheme with neither perturbed term nor additional

boundary condition was proposed in [21]. The energy of this nonlinear scheme decays under a strict constraint on the time step and is bounded when the time step is of the same magnitude of mesh size with the bound depending on the terminal time.

In this paper, we propose a decoupled numerical scheme for the TDGL equations under the temporal gauge

$$(7) \quad \begin{cases} \partial_t \psi + \left(\frac{i}{\kappa} \nabla + \mathbf{A} \right)^2 \psi + (|\psi|^2 - 1) \psi = 0 & \text{in } \Omega \times (0, T] \\ \sigma \partial_t \mathbf{A} + \nabla \times (\nabla \times \mathbf{A}) + \operatorname{Re} \left[\psi^* \left(\frac{i}{\kappa} \nabla + \mathbf{A} \right) \psi \right] = \nabla \times \mathbf{H} & \text{in } \Omega \times (0, T] \end{cases}$$

with the boundary and initial conditions (2). The scheme employs the lowest order of the second type Nedélec element method and the lumped linear element method for spatial discretization of \mathbf{A} and ψ , respectively. For time discretization, the proposed scheme solves \mathbf{A} first by the backward Euler method with the nonlinear term treated explicitly, and then ψ by the lowest order exponential time differencing (ETD) method [1, 5, 19, 20]. The ETD method has been used in many applications to guarantee the discrete MBP. Different from the MBP analysis for real and linear differential equations, the complexity of the order parameter leads to a complex-valued matrix that is not diagonally dominant, and poses difficulty in the MBP analysis for the TDGL equations. By taking full use of the self-adjoint property of the differential operator $(\frac{i}{\kappa} \nabla + \mathbf{A})^2 \psi$ with respect to ψ and the positivity of the intrinsic negative Laplacian operator, the discrete MBP of the proposed scheme is analyzed under a reasonable assumption of triangulations. Compared to the existing numerical schemes in the literature, the proposed scheme preserves the discrete MBP on a triangular mesh without any restrictions on the time step, which is the first decoupled scheme using finite element methods that strictly preserves this property. A similar energy inequality to (6) in continuous level is analyzed for the proposed numerical scheme, which leads to an unconditional energy dissipation law (4) with respect to the original energy (5). This property is of great benefit since it allows the application of adaptive time stepping [30] to significantly speed up long-time simulations. We also analyze the accuracy of the numerical solution, which is verified by numerical examples. The relative low regularity of \mathbf{A}_h and the gradient of ψ_h in the nonlinear terms prevent the error of numerical magnetic potential in L^2 norm to converge at the same rate as the projection error. Nevertheless, the magnetic field $\nabla \times \mathbf{A}$, which is of more physical interest, is proved to admit the same accuracy as the Ritz projection. Besides, a gradient recovery method can be applied to resolve the difficulty brought by the low regularity and nonlinearity, and improve the accuracy of the discrete solutions in L^2 norm numerically.

The organization of this paper is as follows. The decoupled numerical scheme is presented in Section 2. An unconditional energy stability and the discrete MBP for the order parameter are analyzed in Section 3.1 and Section 3.2, respectively. The error estimate of the numerical scheme is proved in Section 4. Some numerical experiments are carried out in Section 5 to verify the theoretical results and demonstrate the performance of the proposed scheme in long-time simulations.

2. FULLY DISCRETE SCHEME FOR THE TDGL EQUATIONS

In this section, we present the fully discrete scheme for the TDGL equation. For simplicity, we introduce some standard notations below. Let \mathbb{C} be the set of complex numbers, $L^2(\Omega, \mathbb{R})$, and $H^1(\Omega, \mathbb{R})$ be the conventional Sobolev spaces defined on a domain $\Omega \subset \mathbb{R}^d$ ($d = 2$ or 3). For any two complex functions $v, w \in L^2(\Omega, \mathbb{C})$, denote the $L^2(\Omega, \mathbb{C})$ inner product and the norm by

$$(v, w) = \int_{\Omega} v w^* dx, \quad \|v\|_0^2 = \int_{\Omega} |v|^2 dx,$$

respectively, where w^* is the conjugate of w and $|v|$ is the magnitude of v . Denote the complex-valued Sobolev spaces

$$H^1(\Omega, \mathbb{C}) = \{\phi = u + iv : u, v \in H^1(\Omega, \mathbb{R}^d)\},$$

and the vector-valued space with d components

$$H(\text{curl}) = \{\mathbf{B} : \mathbf{B} \in L^2(\Omega, \mathbb{R}^d), \nabla \times \mathbf{B} \in L^2(\Omega, \mathbb{R}^d)\}.$$

The weak formulation of the TDGL equations (7) with boundary conditions (2) is specified as follows: find $(\mathbf{A}, \psi) \in H(\text{curl}) \times H^1(\Omega, \mathbb{C})$ such that

$$(8) \quad \begin{cases} (\sigma \partial_t \mathbf{A}, \mathbf{B}) + D(\psi; \mathbf{A}, \mathbf{B}) + (g(\psi), \mathbf{B}) = (\mathbf{H}, \nabla \times \mathbf{B}), & \forall \mathbf{B} \in H(\text{curl}), \\ (\partial_t \psi, \phi) + B(\mathbf{A}; \psi, \phi) - (f_0(\psi), \phi) = 0, & \forall \phi \in H^1(\Omega, \mathbb{C}), \end{cases}$$

with $\mathbf{A}(x, 0) = \mathbf{A}^0(x) \in H(\text{curl})$ and $\psi(x, 0) = \psi^0(x) \in H^1(\Omega, \mathbb{C})$, where

$$(9) \quad \begin{aligned} D(\psi; \mathbf{A}, \mathbf{B}) &= (\nabla \times \mathbf{A}, \nabla \times \mathbf{B}) + (|\psi|^2 \mathbf{A}, \mathbf{B}), & g(\psi) &= \frac{i}{2\kappa} (\psi^* \nabla \psi - \psi \nabla \psi^*), \\ B(\mathbf{A}; \psi, \phi) &= \left(\left(\frac{i}{\kappa} \nabla + \mathbf{A} \right) \psi, \left(\frac{i}{\kappa} \nabla + \mathbf{A} \right) \phi \right), & f_\mu(x) &= (1 - |x|^2)x + \mu x. \end{aligned}$$

Let \mathcal{T}_h be a regular partition of Ω , \mathcal{E}_h be the set of all interior edges of \mathcal{T}_h , \mathbf{t}_e be the unit tangent vector of an edge $e \in \mathcal{E}_h$ and h_K be the diameter of element $K \in \mathcal{T}_h$. Define the mesh size $h = \max_{K \in \mathcal{T}_h} h_K$. Let $P_1(K, \mathbb{C})$ be the set of all polynomials with degrees not larger than one. Define the finite space of the linear element

$$V_h = \{\phi_h \in H^1(\Omega, \mathbb{C}) : \phi_h|_K \in P_1(K, \mathbb{C}), \phi_h \text{ is continuous on any } e \in \mathcal{E}_h\},$$

and the finite space of the lowest order of second kind of Nedélec element by

$$Q_h = \{\mathbf{B}_h \in H(\text{curl}) : \mathbf{B}_h|_K \in P_1(K, \mathbb{R}), \int_e \mathbf{B}_h \cdot \mathbf{t}_e ds \text{ is continuous on any } e \in \mathcal{E}_h\}.$$

Let Π_L be the canonical interpolation operator of the linear element, namely $\Pi_L v(x) = \sum_{i=1}^N v(x_i) \phi_i(x)$, where N is the number of vertices $\{x_i\}_{i=1}^N$ of \mathcal{T}_h , and $\phi_i \in V_h$ is the corresponding basis function with respect to vertex x_i with $\phi_i(x_j) = \delta_{ij}$. Define a diagonal matrix $D = \text{diag}(d_1, \dots, d_N)$ with entries $d_i = |\phi_i|_{0,1,\Omega}$. Denote the inner product $(V, W)_{\mathcal{L}^2} = W^H D V = \sum_{i=1}^N V_i W_i^* |\phi_i|_{0,1,\Omega}$ for any $V, W \in \mathbb{C}^N$, and the operators $I_h : V_h \rightarrow \mathbb{C}^N$ and $\Pi_h : \mathbb{C}^N \rightarrow V_h$ by $I_h w = (w(x_1), \dots, w(x_N))^T$ and $\Pi_h W = \sum_{i=1}^N W_i \phi_i(x)$, respectively. Note that

$$(10) \quad (I_h v, I_h w)_{\mathcal{L}^2} = (\Pi_L(vw^*), 1), \quad \|v\|_0 \lesssim \|I_h v\|_{\mathcal{L}^2} \lesssim \|v\|_0,$$

where the notation $A \lesssim B$ means that there exists a positive constant C , which is independent of the mesh size, such that $A \leq CB$. Define the Ritz projection $R_h \mathbf{A} \in Q_h$ by

$$(11) \quad (\nabla \times (\mathbf{A} - R_h \mathbf{A}), \nabla \times \mathbf{B}_h) + (\mathbf{A} - R_h \mathbf{A}, \mathbf{B}_h) = 0, \quad \forall \mathbf{B}_h \in Q_h,$$

which admits the following error estimate if $\mathbf{A} \in H^2(\Omega, \mathbb{R}^d)$ on a convex domain

$$(12) \quad h \|\nabla \times (I - R_h) \mathbf{A}\|_0 + \|(I - R_h) \mathbf{A}\|_0 \lesssim h^2 |\mathbf{A}|_2.$$

Given a positive integer K_t and time steps $\{\tau_i\}_{i=1}^{K_t}$, we divide the time interval by $\{t_n = \sum_{i=1}^n \tau_i : 0 \leq n \leq K_t\}$ and $T = t_{K_t}$. For any function $F(\cdot, t)$, define $F^n = F(\cdot, t_n)$ and $\partial_t^n F = \partial_t F(\cdot, t_n)$. For any given sequence of functions $\{F^n\}$, denote $d_t^n F = \frac{F^n - F^{n-1}}{\tau_n}$.

Let $\mathbf{A}_h^0 = R_h \mathbf{A}^0$ and $\Psi_h^0 = I_h \psi^0$. Given the approximation $(\mathbf{A}_h^{n-1}, \Psi_h^{n-1}) \in Q_h \times \mathbb{C}^N$ at previous time step t_{n-1} , we first solve the approximation to \mathbf{A}^n by applying the backward Euler method for time discretization and treating the nonlinear terms explicitly. That is to find $\mathbf{A}_h^n \in Q_h$ such that for any $\mathbf{B}_h \in Q_h$,

$$(13) \quad (d_t^n \mathbf{A}_h, \mathbf{B}_h) + D(\Psi_h^{n-1}; \mathbf{A}_h^n, \mathbf{B}_h) = (\mathbf{H}^n, \nabla \times \mathbf{B}_h) - (g(\Psi_h^{n-1}), \mathbf{B}_h),$$

where $\Psi_h^{n-1} = \Pi_h \Psi_h^{n-1}$. We adopt the first order exponential time differencing method (ETD1) with stabilization for time discretization of ψ and the lumped linear element method for spatial discretization by treating the nonlinear terms $B(\mathbf{A}; \psi, \phi)$ and $f_0(\psi)$ in (8) explicitly. To be specific, we seek

$\psi_h^n = u_h(\cdot, t_n) \in V_h$ with $u_h(\cdot, t_{n-1}) = \psi_h^{n-1}$ such that for any $\phi_h \in V_h$ and $t \in [t_{n-1}, t_n]$,

$$(\Pi_L(\partial_t u_h \phi_h^*), 1) + B(\mathbf{A}_h^n; u_h, \phi_h) + \mu_n(\Pi_L(u_h \phi_h^*), 1) - (\Pi_L(f_{\mu_n}(\psi_h^{n-1}) \phi_h^*), 1) = 0,$$

where $\mu_n > 0$ is the stabilization parameter and \mathbf{A}_h^n is known by (13). The matrix form of this formulation reads

$$(14) \quad \begin{cases} \frac{d}{dt} U_h(t) = L_{\mu_n, h}^n U_h(t) + f_{\mu_n}(\Psi_h^{n-1}), & \forall t \in [t_{n-1}, t_n], \\ U_h(t_{n-1}) = \Psi_h^{n-1}, \end{cases}$$

where $U_h(t) = I_h u_h(\cdot, t) \in \mathbb{C}^N$ and the entries of the complex matrix $L_{\mu_n, h}^n$ are

$$(15) \quad L_{\mu_n, h}^n = D^{-1} \hat{L}^n - \mu_n I, \quad \text{with} \quad (\hat{L}^n)_{ij} = -B(\mathbf{A}_h^n; \phi_j, \phi_i).$$

Since the diagonal matrix D is positive definite and the Hermitian matrix \hat{L}^n is negative definite, $L_{\mu_n, h}^n$ is negative definite for any $\mu_n > 0$, i.e.

$$(16) \quad W^* L_{\mu_n, h}^n W \leq -\mu_n W^* W, \quad \forall W \in \mathbb{C}^N.$$

An equivalent form of the equation (14) is

$$(17) \quad \Psi_h^n = \phi_0(\tau_n L_{\mu_n, h}^n) \Psi_h^{n-1} - \tau_n \phi_1(\tau_n L_{\mu_n, h}^n) f_{\mu_n}(\Psi_h^{n-1}),$$

where $\phi_0(a) = e^a$ and $\phi_1(a) = \frac{1-e^a}{a}$ for $a \neq 0$. Since the matrix $L_{\mu_n, h}^n$ varies in different time intervals, we use the Krylov iteration method in [28] to compute the exponential integral in (17).

3. DISCRETE ENERGY STABILITY AND MAXIMUM BOUND PRINCIPLE

In this section, we will show that the proposed scheme (13) with (14) inherits the energy dissipation law (4) and the maximum bound principle (3) in the discrete sense.

3.1. Discrete energy stability. Define the discrete energy G_h^n by

$$G_h^n = \frac{1}{2} \left\| \left(\frac{i}{\kappa} \nabla + \mathbf{A}_h^n \right) \psi_h^n \right\|_0^2 + \frac{1}{2} \left\| \nabla \times \mathbf{A}_h^n - \mathbf{H}^n \right\|_0^2 + \frac{1}{4} \left\| |\Psi_h^n|^2 - 1 \right\|_{\ell^2}^2.$$

and $\mathbf{M}_h^n = \frac{1}{4\pi} (\nabla \times \mathbf{A}_h^n - \mathbf{H}^n)$ in a similar form to (5).

Theorem 1. For any positive $\{\tau_n\}_{n=1}^{K_t}$, the solution $\{(\mathbf{A}_h^n, \psi_h^n)\}_{n=0}^{K_t}$ generated by the discrete system (13) and (14) with $\mu_n \geq 1$ satisfies the energy inequality

$$d_t^n G_h + \|d_t^n \mathbf{A}_h\|_0^2 + (\mu_n - 1) \tau_n \|d_t^n \Psi_h\|_{\ell^2}^2 \leq -4\pi (\mathbf{M}_h^n, d_t^n \mathbf{H}), \quad \forall 1 \leq n \leq K_t.$$

If \mathbf{H} is independent of t and $\mu_n \geq 1$,

$$G_h^n \leq G_h^{n-1}, \quad \forall 1 \leq n \leq K_t,$$

i.e., the proposed scheme is unconditionally energy stable.

Proof. The difference between discrete energy at two consecutive time levels yields

$$d_t^n G_h = \frac{1}{2} d_t^n \left\| \left(\frac{i}{\kappa} \nabla + \mathbf{A}_h \right) \psi_h \right\|_0^2 + \frac{1}{2} d_t^n \|4\pi \mathbf{M}_h\|_0^2 + \frac{1}{4} d_t^n \left\| |\Psi_h|^2 - 1 \right\|_{\ell^2}^2.$$

It follows (9) that $d_t^n \left\| \left(\frac{i}{\kappa} \nabla + \mathbf{A}_h \right) \psi_h \right\|_0^2 = \frac{1}{\tau_n} (B(\mathbf{A}_h^n, \psi_h^n, \psi_h^n) - B(\mathbf{A}_h^{n-1}, \psi_h^{n-1}, \psi_h^{n-1}))$, therefore,

$$(18) \quad \frac{1}{2} d_t^n \left\| \left(\frac{i}{\kappa} \nabla + \mathbf{A}_h \right) \psi_h \right\|_0^2 = \frac{1}{2\tau_n} \left(B(\mathbf{A}_h^n, \psi_h^n, \psi_h^n) - B(\mathbf{A}_h^n, \psi_h^{n-1}, \psi_h^{n-1}) \right) + \frac{1}{2} (d_t^n |\mathbf{A}_h|^2, |\psi_h^{n-1}|^2) + (g(\psi_h^{n-1}), d_t^n \mathbf{A}_h).$$

Note that $\frac{1}{2} d_t^n |u|^2 = \text{Re}(u^n, d_t^n u) - \frac{\tau_n}{2} |d_t^n u|^2$ for any u^{n-1} and u^n . Thus,

$$(19) \quad (\mathbf{M}^n, d_t^n \mathbf{M}_h) = \frac{1}{2} d_t^n \|\mathbf{M}_h\|^2 + \frac{\tau_n}{2} \|d_t^n \mathbf{M}_h\|^2.$$

Let $\mathbf{B}_h = d_t^n \mathbf{A}_h$ in the scheme (13). It holds that

$$\|d_t^n \mathbf{A}_h\|_0^2 + (4\pi \mathbf{M}_h^n, 4\pi d_t^n \mathbf{M}_h + d_t^n \mathbf{H}) + (|\psi_h^{n-1}|^2 \mathbf{A}_h^n, d_t^n \mathbf{A}_h) = -(g(\psi_h^{n-1}), d_t^n \mathbf{A}_h).$$

A summation of (18), (19) and the equation above yields

$$\begin{aligned} & \frac{1}{2} d_t^n \left\| \left(\frac{i}{\kappa} \nabla + \mathbf{A}_h \right) \psi_h \right\|_0^2 + \frac{1}{2} d_t^n \|4\pi \mathbf{M}_h\|_0^2 + \|d_t^n \mathbf{A}_h\|_0^2 + \frac{\tau_n}{2} \|4\pi d_t^n \mathbf{M}_h\|_0^2 \\ &= \frac{1}{2\tau_n} \left(B(\mathbf{A}_h^n, \psi_h^n, \psi_h^n) - B(\mathbf{A}_h^n, \psi_h^{n-1}, \psi_h^{n-1}) \right) - (4\pi \mathbf{M}_h^n, d_t^n \mathbf{H}) - (|\psi_h^{n-1}|^2 \mathbf{A}_h^n, d_t^n \mathbf{A}_h) + \frac{1}{2} (d_t^n |\mathbf{A}_h|^2, |\psi_h^{n-1}|^2). \end{aligned}$$

Note that $(|\psi_h^{n-1}|^2 \mathbf{A}_h^n, d_t^n \mathbf{A}_h) - \frac{1}{2} (d_t^n |\mathbf{A}_h|^2, |\psi_h^{n-1}|^2) = \frac{\tau_n}{2} \| |\psi_h^{n-1}| d_t^n \mathbf{A}_h \|_0^2 \geq 0$ and

$$B(\mathbf{A}_h^n, \phi_h, \phi_h) = -(I_h \phi_h)^H \hat{L}^n (I_h \phi_h) = (L_{0,h}^n (I_h \phi_h), I_h \phi_h)_{\ell^2}$$

for any $\phi_h \in V_h$. It follows that

$$\begin{aligned} (20) \quad & \frac{1}{2} d_t^n \left\| \left(\frac{i}{\kappa} \nabla + \mathbf{A}_h \right) \psi_h \right\|_0^2 + \frac{1}{2} d_t^n \|4\pi \mathbf{M}_h\|_0^2 + \|d_t^n \mathbf{A}_h\|_0^2 + \frac{\tau_n}{2} \|4\pi d_t^n \mathbf{M}_h\|_0^2 \\ & \leq -\frac{1}{2\tau_n} \left((L_{0,h}^n \Psi_h^n, \Psi_h^n)_{\ell^2} - (L_{0,h}^n \Psi_h^{n-1}, \Psi_h^{n-1})_{\ell^2} \right) - (4\pi \mathbf{M}_h^n, d_t^n \mathbf{H}). \end{aligned}$$

By (16),

$$\begin{aligned} (21) \quad & - \left((L_{0,h}^n \Psi_h^n, \Psi_h^n)_{\ell^2} - (L_{0,h}^n \Psi_h^{n-1}, \Psi_h^{n-1})_{\ell^2} \right) \\ & = -2\tau_n \operatorname{Re} (L_{0,h}^n \Psi_h^n, d_t^n \Psi_h)_{\ell^2} + \tau_n^2 \operatorname{Re} (L_{0,h}^n d_t^n \Psi_h, d_t^n \Psi_h)_{\ell^2} \leq -2\tau_n \operatorname{Re} (L_{0,h}^n \Psi_h^n, d_t^n \Psi_h)_{\ell^2}. \end{aligned}$$

Suppose a and b are complex numbers and $|a| \leq 1, |b| \leq 1$, it holds that

$$\frac{1}{4} ((a^2 - 1)^2 - (b^2 - 1)^2) \leq (b^2 - 1) \operatorname{Re}(b^*(a - b)) + (a - b)^*(a - b),$$

which implies that for any $\mu_n \geq 1$,

$$(22) \quad \frac{1}{4} d_t^n \| |\Psi_h|^2 - 1 \|_{\ell^2}^2 + (\mu_n - 1) \tau_n \|d_t^n \Psi_h\|_{\ell^2}^2 \leq \operatorname{Re}(\mu_n \Psi_h^n - f_{\mu_n}(\Psi_h^{n-1}), d_t^n \Psi_h)_{\ell^2}.$$

Substituting (21) and (22) into (20) yields

$$\begin{aligned} (23) \quad & d_t^n G_h + \|d_t^n \mathbf{A}_h\|_0^2 + (\mu_n - 1) \tau_n \|d_t^n \Psi_h\|_{\ell^2}^2 + \frac{\tau_n}{2} \|d_t^n (\nabla \times \mathbf{A}_h - \mathbf{H})\|_0^2 \\ & \leq -\operatorname{Re}(f_{\mu_n}(\Psi_h^{n-1}) + L_{\mu_n,h}^n \Psi_h^n, d_t^n \Psi_h)_{\ell^2} - (4\pi \mathbf{M}_h^n, d_t^n \mathbf{H}). \end{aligned}$$

The ETD1 scheme in (17) indicates that

$$\begin{aligned} f_{\mu_n}(\Psi_h^{n-1}) &= - (1 - e^{L_{\mu_n,h}^n \tau_n})^{-1} L_{\mu_n,h}^n (\Psi_h^n - e^{L_{\mu_n,h}^n \tau_n} \Psi_h^{n-1}) \\ &= - (1 - e^{L_{\mu_n,h}^n \tau_n})^{-1} L_{\mu_n,h}^n (\Psi_h^n - \Psi_h^{n-1} + (I - e^{L_{\mu_n,h}^n \tau_n}) \Psi_h^{n-1}) \\ &= -\tau_n (1 - e^{L_{\mu_n,h}^n \tau_n})^{-1} L_{\mu_n,h}^n d_t^n \Psi_h - L_{\mu_n,h}^n \Psi_h^{n-1}. \end{aligned}$$

Define $g(x) = -x + \frac{x}{1 - e^x}$ and the operator $\Delta_1 = g_1(L_{\mu_n,h}^n \tau_n)$. It follows that

$$-L_{\mu_n,h}^n \Psi_h^n - f_{\mu_n}(\Psi_h^{n-1}) = \Delta_1 (d_t^n \Psi_h).$$

Since $g(x) < 0$ for all $x < 0$ and $L_{\mu_n,h}^n$ is self-adjoint and negative definite, the operator Δ_1 is also negative definite. Thus, $-\operatorname{Re}(f_{\mu_n}(\Psi_h^{n-1}) + L_{\mu_n,h}^n \Psi_h^n, d_t^n \Psi_h) \leq 0$. A combination of this and (23) gives

$$d_t^n G_h + \|d_t^n \mathbf{A}_h\|_0^2 + (\mu_n - 1) \tau_n \|d_t^n \Psi_h\|_{\ell^2}^2 + \frac{\tau_n}{2} \|4\pi d_t^n \mathbf{M}_h\|_0^2 \leq -(4\pi \mathbf{M}_h^n, d_t^n \mathbf{H}).$$

If \mathbf{H} is stationary, the right hand side of the above inequality equals zero, which indicates $G_h^n \leq G_h^{n-1}$, and completes the proof. \square

Remark 1. The TDGL equations (7) is an L^2 gradient flow of the Gibbs energy with the energy of solution remaining almost the same after a certain time. The unconditional energy decay property allows the application of the adaptive time stepping strategy in [30] to speed up long time simulations.

3.2. Discrete Maximum Bound Principle. In this section, we consider the discrete MBP for the proposed decoupled scheme (13) and (14). To begin with, we consider an ODE system taking the form

An analytical framework is proposed in [10] for some sufficient conditions that lead to a maximum bound principle for the system

$$(24) \quad \frac{du}{dt} + \mu u = Lu + N[u] \quad \text{with} \quad u(0, x) = u^0(x)$$

with real-valued L and $N(\xi) = \mu\xi + h(\xi)$. This framework can be extended to complex-valued systems, which of a finite dimensional system is presented below.

Lemma 1. Given any constant $T > 0$, assume that

- (1) for any $U \in \mathbb{C}^N$, it holds that $\text{Re}(U_i^*(LU)_i) < 0$ if $|U_i| = \max_{1 \leq j \leq N} |U_j|$;
- (2) there exists $\lambda_0 > 0$ such that $\lambda_0 I - L$ is reversible,
- (3) $|N(\xi)| \leq \mu\beta$ for any $|\xi| \leq \beta$ and $|N(\xi_1) - N(\xi_2)| \leq 2\mu|\xi_1 - \xi_2|$ for any $|\xi_1| \leq \beta$ and $|\xi_2| \leq \beta$.

If $\|u^0\|_{L^\infty} \leq \beta$ and $\mu \geq \max_{|\xi| \leq \beta} |h'(\xi)|$, it satisfies $\|u(t)\|_{L^\infty} \leq \beta$ for all $t \in [0, T]$.

Assumption (1) and (2) in the above lemma indicate that the linear operator $L_{\mu_n, h}^n$ is the generator of a contraction semigroup since Assumption (1) implies

$$\|(\lambda I - L_{\mu_n, h}^n)U\|_{\ell^\infty}^2 \geq |\lambda U_i - (L_{\mu_n, h}^n U)_i|^2 = \lambda^2 |U_i|^2 + |(L_{\mu_n, h}^n U)_i|^2 - 2\text{Re}(U_i^*(LU)_i) > \lambda \|U\|_{\ell^\infty}^2.$$

Lemma 1 follows directly from this fact and the analysis in [10] with the proof omitted here.

Notice that for real-valued systems, the first assumption reduces to $U_i^*(LU)_i \leq 0$ if $|U_i| = \max_{1 \leq j \leq N} |U_j|$ for any $U \in \mathbb{R}^N$, which is exactly the assumption in [10] for real-valued systems. It is widely used in MBP analysis of numerical schemes using ETD methods that if all the diagonal entries of a strictly diagonally dominant matrix L are negative, Assumption (1) holds for the real-valued system. For complex-valued systems, if L is a Hermitian matrix with negative entries on the diagonal and strictly diagonally dominant, Assumption (1) still holds.

In this paper, we consider the discrete MBP of the proposed scheme when the triangulation satisfies the following assumption.

Assumption 1. The triangulation is shape regular and quasi-uniform, where all the interior angles ($d = 2$) or interior angles of faces ($d = 3$) are acute.

By Lemma 1, the key to analyzing discrete MBP for the ETD1 scheme (14) is to prove that $L_{\mu_n, h}^n$ is a generator of a contraction semigroup, namely

$$(25) \quad \text{Re}(U_i^*(L_{\mu_n, h}^n U)_i) < 0, \quad \text{for some } i \in \{1, \dots, N\}$$

holds for any $U \in \mathbb{C}^N$. Note that even though the real part of the matrix $L_{0, h}^n$ is diagonally dominant, the matrix itself is not necessarily weakly diagonally dominant. To derive the discrete MBP for the proposed scheme, we need to look into the properties of the linear operator $L_{\mu_n, h}^n$. Denote the entries of $L_{\mu_n, h}^n \in \mathbb{C}^{N \times N}$ by $(L_{ij})_{i, j=1}^N$ with $L_{ij} = L_{ij}^r + iL_{ij}^i$ and

$$(26) \quad \begin{aligned} L_{ij}^r &= \frac{1}{d_i} \left(-\frac{1}{\kappa^2} \int_{\Omega} \nabla \phi_j \cdot \nabla \phi_i \, dx - \int_{\Omega} |\mathbf{A}_h^n|^2 \phi_i \phi_j \, dx - \mu_n \delta_{ij} |\phi_i|_{0,1,\Omega} \right), \\ L_{ij}^i &= \frac{1}{\kappa d_i} \int_{\Omega} \mathbf{A}_h^n \cdot (\phi_j \nabla \phi_i - \phi_i \nabla \phi_j) \, dx, \end{aligned}$$

where $d_i = |\phi_i|_{0,1,\Omega}$. It follows Assumption 1 that there exists positive constants C_1, C_2 and C_3 , which are independent on the mesh size, such that for any $i \neq j$,

$$\int_{\Omega} \nabla \phi_j \cdot \nabla \phi_i \, dx \leq -C_1 h^{d-2}, \quad |\kappa d_i L_{ij}^i| \leq C_2 h^{d-1} \|\mathbf{A}_h^n\|_{\infty}, \quad |\phi_i|_{0,1,\Omega} \geq C_3 h^d.$$

For any $1 \leq i, j \leq N$, define vector $\vec{v}_{ij} = (a_{ij}, b_{ij}, c_{ij})$ by

$$a_{ij} = -\frac{h^{2-d}}{\kappa^2} \int_{\Omega} \nabla \phi_j \cdot \nabla \phi_i dx, \quad b_{ij} = d_i h^{1-d} L_{ij}^i, \quad c_{ij} = \tilde{\mu}_1 h^{-d} |\phi_i|_{0,1,\Omega},$$

where constant $\tilde{\mu}_1$ is to be determined later. It follows that each entry of the vector \vec{v}_{ij} is independent of the mesh size h and

$$(27) \quad a_{ij} \geq \frac{C_1}{\kappa^2}, \quad 0 \leq |b_{ij}| \leq \frac{C_2}{\kappa} \|\mathbf{A}_h^n\|_{\infty}, \quad c_{ij} \geq \tilde{\mu}_1 C_3.$$

The following theorem shows that the operator $L_{\mu_n, h}^n$ is the generator of a contraction semigroup and the discrete MBP holds for the proposed scheme when the stabilization parameter $\mu_n > (\frac{C_2^2}{2C_1C_3} + \frac{3}{8}) \|\mathbf{A}_h^n\|_{\infty}^2$, where the constants C_1, C_2 and C_3 are independent on the mesh size h , Ginzburg-Landau parameter κ and \mathbf{A}_h^n is known by (14).

Theorem 2. *Assume that the matrix $L_{\mu_n, h}^n$ is assembled with $\mu_n > (\frac{C_2^2}{2C_1C_3} + \frac{3}{8}) \|\mathbf{A}_h^n\|_{\infty}^2$ and Assumption 1 holds. Then the discrete MBP holds, i.e.*

$$\|\Psi_h^n\|_{\ell^{\infty}} \leq 1, \quad \text{if} \quad \|\psi^0\|_{\infty} \leq 1.$$

Proof. Define a matrix $T \in \mathbb{C}^{N \times N}$ with entries $T_{ij} = U_i^* U_j = T_{ij}^r + iT_{ij}^i$. Then,

$$(28) \quad \text{Re}(U_i^* \sum_{j=1}^N L_{ij} U_j) = L_{ii}^r T_{ii}^r + \sum_{j \neq i} (L_{ij}^r T_{ij}^r - L_{ij}^i T_{ij}^i).$$

It follows $\sum_{i=1}^N \phi_i(x) = 1$, $\sum_{i=1}^N \nabla \phi_i(x) = 0$ and (26) that

$$(29) \quad L_{ii}^r = \frac{1}{d_i} \left(\frac{1}{\kappa^2} \sum_{j \neq i} \int_{\Omega} \nabla \phi_j \cdot \nabla \phi_i dx - \int_{\Omega} |\mathbf{A}_h^n|^2 \phi_i^2 dx - \mu_n |\phi_i|_{0,1,\Omega} \right).$$

Substituting (26) and (29) into (28) yields

$$(30) \quad \text{Re}(U_i^* \sum_{j=1}^N L_{ij} U_j) = \frac{1}{d_i} (R_i^1 + R_i^2),$$

where the stabilization parameter $\mu_n = \tilde{\mu}_1 + \tilde{\mu}_2$ is to be determined later and

$$R_i^1 = - \sum_{j \neq i} \ell_i(U_j; \vec{v}_{ij}), \quad \text{with} \quad \ell_i(U_j; \vec{v}_{ij}) = a_{ij} h^{d-2} (T_{ii}^r - T_{ij}^r) + b_{ij} h^{d-1} T_{ij}^i + c_{ij} h^d T_{ii}^r,$$

$$R_i^2 = - \sum_{j=1}^N \int_{\Omega} |\mathbf{A}_h^n|^2 \phi_i \phi_j dx T_{ij}^r - \tilde{\mu}_2 |\phi_i|_{0,1,\Omega} T_{ii}^r.$$

Let (r_j, θ_j) be the polar coordinates of U_j . We can find $i \in \{1, \dots, N\}$ such that $r_i = \max_{1 \leq j \leq N} r_j$. Then, $T_{ii} - T_{ij} = r_i^2 - r_i r_j e^{i(\theta_j - \theta_i)}$. Note that

$$\ell_i(U_j; \vec{v}_{ij}) = a_{ij} r_i^2 h^{d-2} - a_{ij} r_i r_j h^{d-2} \cos(\theta_j - \theta_i) - b_{ij} r_i r_j h^{d-1} \sin(\theta_j - \theta_i) + c_{ij} r_i^2 h^d$$

$$\geq h^{d-2} (a_{ij} r_i^2 - r_i r_j \sqrt{a_{ij}^2 + b_{ij}^2} h^2 + c_{ij} r_i^2 h^2).$$

The inequality (27) indicates that a_{ij} is positive. Since $\sqrt{a_{ij}^2 + b_{ij}^2} h^2 \leq a_{ij} + \frac{b_{ij}^2 h^2}{2a_{ij}}$,

$$(31) \quad \ell_i(U_j; \vec{v}_{ij}) \geq a_{ij} r_i^2 h^{d-2} - a_{ij} r_i r_j h^{d-2} + (c_{ij} - \frac{b_{ij}^2}{2a_{ij}}) r_i^2 h^d \geq (c_{ij} - \frac{b_{ij}^2}{2a_{ij}}) r_i^2 h^d,$$

and the equation holds only if $r_i = r_j$ and $b_{ij} = 0$. It follows that

$$(32) \quad R_i^1 = - \sum_{j \neq i} \ell_i(U_j; \vec{v}_{ij}) \leq - \sum_{j \neq i} (c_{ij} - \frac{b_{ij}^2}{2a_{ij}}) r_i^2 h^2.$$

When $\tilde{\mu}_1 > \frac{C_2^2 \|A_h^n\|_\infty^2}{2C_1 C_3}$, it follows (27) that $c_{ij} - \frac{b_{ij}^2}{2a_{ij}} > 0$, which implies that

$$(33) \quad R_i^1 = - \sum_{j \neq i} \ell_i(U_j; \vec{v}_{ij}) < 0.$$

Since $\phi_i \geq 0$ and $\sum_{j \neq i} \phi_j = 1 - \phi_i$,

$$\begin{aligned} R_i^2 &\leq \sum_{j \neq i} \int_{\Omega} |A_h^n|^2 \phi_i \phi_j dx T_{ii}^r - \int_{\Omega} |A_h^n|^2 \phi_i^2 dx T_{ii}^r - \tilde{\mu}_2 |\phi_i|_{0,1,\Omega} T_{ii}^r \\ &= \int_{\Omega} (-2|A_h^n|^2 (\phi_i - \frac{1}{4})^2 - (\tilde{\mu}_2 \phi_i - \frac{1}{8} |A_h^n|^2)) dx T_{ii}^r. \end{aligned}$$

It follows from $T_{ii}^r > 0$ and $\int_K \phi_i dx = \frac{|K|}{3}$ that $R_i^2 \leq 0$ if $\tilde{\mu}_2 \geq \frac{3}{8} \|A_h^n\|_\infty^2$. A substitution of this and (33) into (30) leads to $\text{Re}(U_i^* \sum_{j=1}^N L_{ij} U_j) < 0$, which verifies the assumption (1) in Lemma 1. Assumption (2) holds following the negative definite property (16) of the matrix $L_{\mu_n, h}^n$. For any $x_1, x_2 \in \mathbb{C}$ with the magnitude not larger than 1, it is easy to verify that $|f_{\mu_n}(x_1) - f_{\mu_n}(x_2)| \leq 2\mu_n |x_1 - x_2|$. As proved in [9],

$$|f_{\mu_n}(x_1)| = f_{\mu_n}(|x_1|) \leq \mu_n \quad \text{if } \mu_n \geq 2,$$

which verifies the assumption (3) in Lemma 1 with $\beta = 1$ and completes the proof. \square

4. ERROR ESTIMATE

In this section, we will analyze the convergence of the numerical solutions by the proposed scheme under the regularity assumption below.

Assumption 2. Assume that Ω is a convex polygon (or polyhedron). The solution of the initial boundary value problem (7) with (2) satisfies the regularity conditions

$$\begin{aligned} \psi, \partial_t \psi &\in L^\infty(0, T; H^2(\Omega, \mathbb{C})), \quad \mathbf{A}, \partial_t \mathbf{A} \in L^\infty(0, T; H^2(\Omega, \mathbb{R})), \\ \partial_{tt} \mathbf{A} &\in L^\infty(0, T; H^1(\Omega, \mathbb{R})). \end{aligned}$$

To begin with, we explore the relation between the errors $e_{\mathbf{A}}^n$ and E_{ψ}^n at two consecutive time levels by use of the error equations, where

$$e_{\mathbf{A}}^j = \mathbf{A}_h^j - R_h \mathbf{A}^j, \quad E_{\psi}^j = \Psi_h^j - I_h \psi^j, \quad e_{\psi}^j = \Pi_h E_{\psi}^j.$$

By the estimate (12) and the interpolation error of the linear element

$$(34) \quad \|\mathbf{A}^n - R_h \mathbf{A}^n\|_0 + h \|\nabla \times (\mathbf{A}^n - R_h \mathbf{A}^n)\|_0 + \|\psi - \Pi_L \psi\|_0 + h \|\nabla(\psi - \Pi_L \psi)\|_0 \lesssim h^2.$$

Lemma 2. Assume that Assumption 1 and 2 hold. Let $\mathbf{A}_h^0 = R_h \mathbf{A}^0$ and $\Psi_h^0 = I_h \psi^0$ with $\|\psi^0\|_\infty \leq 1$. The approximating solution $\{(\mathbf{A}_h^n, \Psi_h^n)\}_{n=1}^{K_t}$ is generated by the discrete system (13) and (14) with the stabilizing parameter $\mu_n \geq \max\{(\frac{C_2^2}{2C_1 C_3} + \frac{3}{8}) \|A_h^n\|_\infty^2, 2\}$ and uniform time step $\tau_n = \tau$. For any $1 \leq n \leq K_t$,

$$(35) \quad \sigma \|e_{\mathbf{A}}^n\|^2 + 2\tau \|\nabla \times e_{\mathbf{A}}^n\|_0^2 \leq \sigma(1 + C\tau) \|e_{\mathbf{A}}^{n-1}\|^2 + \tau \|(\frac{i}{\kappa} \nabla + \mathbf{A}_h^{n-1}) e_{\psi}^{n-1}\|_0^2 + C\tau (\|E_{\psi}^{n-1}\|_{\ell^2}^2 + h^2 + \tau^2),$$

$$(36) \quad \|\nabla \times e_{\mathbf{A}}^n\|_0^2 \leq \|\nabla \times e_{\mathbf{A}}^{n-1}\|_0^2 + C\tau (\|(\frac{i}{\kappa} \nabla + \mathbf{A}_h^{n-1}) e_{\psi}^{n-1}\|_0^2 + \|e_{\mathbf{A}}^{n-1}\|_0^2 + \|e_{\mathbf{A}}^n\|_0^2 + \|E_{\psi}^{n-1}\|_{\ell^2}^2 + h^2 + \tau^2).$$

Proof. By the definition of the Ritz projection R_h in (11) and (13),

$$(37) \quad \begin{aligned} & \sigma(d_t^n e_A, \mathbf{B}_h) + (\nabla \times e_{\mathbf{A}}^n, \nabla \times \mathbf{B}_h) + (\operatorname{Re}[(\psi_h^{n-1})^* (\frac{i}{\kappa} \nabla + \mathbf{A}_h^n) \psi_h^{n-1} - (\psi^n)^* (\frac{i}{\kappa} \nabla + \mathbf{A}^n) \psi^n], \mathbf{B}_h) \\ &= \sigma(\partial_t^n \mathbf{A} - d_t^n \mathbf{A}, \mathbf{B}_h) + \sigma((I - R_h) d_t^n \mathbf{A}, \mathbf{B}_h) - ((I - R_h) \mathbf{A}^n, \mathbf{B}_h). \end{aligned}$$

Since $\partial_t^n \mathbf{A} - d_t^n \mathbf{A} = \frac{1}{\tau} \int_{t_{n-1}}^{t_n} \partial_t^n \mathbf{A} - \partial_t \mathbf{A}(s) ds$,

$$(38) \quad |(\partial_t^n \mathbf{A} - d_t^n \mathbf{A}, \mathbf{B}_h)| \lesssim \tau \|\mathbf{B}_h\|_0.$$

By the estimate (12),

$$(39) \quad |\sigma((I - R_h) d_t^n \mathbf{A}, \mathbf{B}_h)| + |((I - R_h) \mathbf{A}^n, \mathbf{B}_h)| \lesssim h^2 \|\mathbf{B}_h\|_0.$$

Note that

$$\begin{aligned} & (\psi_h^{n-1})^* (\frac{i}{\kappa} \nabla + \mathbf{A}_h^n) \psi_h^{n-1} - (\psi^n)^* (\frac{i}{\kappa} \nabla + \mathbf{A}^n) \psi^n \\ &= (e_\psi^{n-1})^* (\frac{i}{\kappa} \nabla + \mathbf{A}^n) \Pi_L \psi^{n-1} + (\psi_h^{n-1})^* (\frac{i}{\kappa} \nabla + \mathbf{A}^n) e_\psi^{n-1} + (\psi_h^{n-1})^* (\mathbf{A}_h^n - \mathbf{A}^n) \psi_h^{n-1} \\ & \quad + (\Pi_L \psi^{n-1})^* (\frac{i}{\kappa} \nabla + \mathbf{A}^n) \Pi_L \psi^{n-1} - (\psi^n)^* (\frac{i}{\kappa} \nabla + \mathbf{A}^n) \psi^n, \end{aligned}$$

where Assumption 2 and the error estimates in (34) and (12) imply that

$$\begin{aligned} & |(e_\psi^{n-1})^* (\frac{i}{\kappa} \nabla + \mathbf{A}^n) \Pi_L \psi^{n-1}, \mathbf{B}_h| \lesssim \|e_\psi^{n-1}\|_0 \|\mathbf{B}_h\|_0. \\ & |((\psi_h^{n-1})^* (\frac{i}{\kappa} \nabla + \mathbf{A}^n) e_\psi^{n-1}, \mathbf{B}_h)| \leq \|(\frac{i}{\kappa} \nabla + \mathbf{A}^n) e_\psi^{n-1}\|_0 \|\mathbf{B}_h\|_0 \|\psi_h^{n-1}\|_\infty \\ & |((\psi_h^{n-1})^* (\mathbf{A}_h^n - \mathbf{A}^n) \psi_h^{n-1}, \mathbf{B}_h)| \leq (\|e_{\mathbf{A}}^n\|_0 + Ch^2) \|\mathbf{B}_h\|_0 \|\psi_h^{n-1}\|_\infty^2 \\ & |((\Pi_L \psi^{n-1})^* (\frac{i}{\kappa} \nabla + \mathbf{A}^n) \Pi_L \psi^{n-1} - (\psi^n)^* (\frac{i}{\kappa} \nabla + \mathbf{A}^n) \psi^n, \mathbf{B}_h)| \lesssim (\tau + h) \|\mathbf{B}_h\|_0. \end{aligned}$$

By Theorem 2, $\|\psi_h^{n-1}\|_\infty \leq 1$. It follows that

$$(40) \quad \begin{aligned} & |(\operatorname{Re}[(\psi_h^{n-1})^* (\frac{i}{\kappa} \nabla + \mathbf{A}_h^n) \psi_h^{n-1} - (\psi^n)^* (\frac{i}{\kappa} \nabla + \mathbf{A}^n) \psi^n], \mathbf{B}_h)| \\ & \leq \left(\|(\frac{i}{\kappa} \nabla + \mathbf{A}^n) e_\psi^{n-1}\|_0 + \|e_{\mathbf{A}}^n\|_0 + C \|e_\psi^{n-1}\|_0 + C\tau + Ch \right) \|\mathbf{B}_h\|_0. \end{aligned}$$

It follows from $\|e_\psi^{n-1}\|_\infty \leq \|I_h \psi^{n-1}\|_\infty + \|\psi_h^{n-1}\|_\infty \leq 2$ and (12) that

$$\begin{aligned} & \|(\frac{i}{\kappa} \nabla + \mathbf{A}^n) e_\psi^{n-1}\|_0 \leq \|(\frac{i}{\kappa} \nabla + \mathbf{A}_h^{n-1}) e_\psi^{n-1}\|_0 + \|(\mathbf{A}^n - \mathbf{A}_h^{n-1}) e_\psi^{n-1}\|_0 \\ & \leq \|(\frac{i}{\kappa} \nabla + \mathbf{A}_h^{n-1}) e_\psi^{n-1}\|_0 + 2 \|e_{\mathbf{A}}^{n-1}\|_0 + C(\tau + h^2). \end{aligned}$$

Let $\mathbf{B}_h = e_{\mathbf{A}}^n$ in (37). By Young's inequality, a combination of (37), (38), (39), (40) and this leads to

$$\sigma \|e_{\mathbf{A}}^n\|^2 + 2\tau \|\nabla \times e_{\mathbf{A}}^n\|_0^2 \leq \sigma(1 + C\tau) \|e_{\mathbf{A}}^{n-1}\|^2 + \tau \|(\frac{i}{\kappa} \nabla + \mathbf{A}_h^{n-1}) e_\psi^{n-1}\|_0^2 + C\tau (\|e_\psi^{n-1}\|_0^2 + \tau^2 + h^2).$$

Let $\mathbf{B}_h = d_t^n e_{\mathbf{A}}$ in (37). A similar analysis yields

$$\|\nabla \times e_{\mathbf{A}}^n\|_0^2 \leq \|\nabla \times e_{\mathbf{A}}^{n-1}\|_0^2 + C\tau (\|(\frac{i}{\kappa} \nabla + \mathbf{A}_h^{n-1}) e_\psi^{n-1}\|_0^2 + \|e_{\mathbf{A}}^{n-1}\|_0^2 + \|e_{\mathbf{A}}^n\|_0^2 + \|e_\psi^{n-1}\|_0^2 + \tau^2 + h^2),$$

which completes the proof. \square

Given any $\mu \geq 0$ and $\mathbf{B} \in H^1(\Omega)$, denote the linear operator $L_\mu[\mathbf{B}]\psi = -(\frac{i}{\kappa}\nabla + \mathbf{B})^2\psi - \mu\psi$. The matrix $L_{\mu_n, h}^n$ in (14) relates to a spatial discretization of the operator $L_{\mu_n}[\mathbf{A}^n]$. Let $S_\psi(t) = U_h(t) - \Psi(t)$ with U_h defined in (14) and $\Psi(t) = I_h\psi(\cdot, t)$. A subtraction of (14) from (7) reads

$$(41) \quad \begin{cases} \frac{d}{dt}S_\psi = L_{\mu_n, h}^n S_\psi + \delta_n^1 + \delta_n^2 + \delta_n^3 + f_{\mu_n}(\Psi_h^{n-1}) - f_{\mu_n}(I_h\psi^{n-1}), & t \in [t_{n-1}, t_n], \\ S_\psi(t_{n-1}) = E_\psi^{n-1}, \end{cases}$$

where

$$(42) \quad \begin{aligned} \delta_n^1 &= L_{\mu_n, h}^n I_h\psi - I_h L_{\mu_n}[\mathbf{A}^n]\psi, & \delta_n^2 &= I_h(L_{\mu_n}[\mathbf{A}^n] - L_{\mu_n}[\mathbf{A}])\psi, \\ \delta_n^3 &= f_{\mu_n}(I_h\psi^{n-1}) - f_{\mu_n}(I_h\psi). \end{aligned}$$

The first term δ_n^1 represents the consistency error of the numerical scheme and the other two terms relates to the error in time discretization.

Lemma 3. *Under Assumption 2, it holds for any $W_h \in \mathbb{C}^N$ that*

$$|(\delta_n^1, W_h)_{\mathcal{L}^2}| \lesssim (\|e_{\mathbf{A}}^n\|_0 + h) \left(\left\| \left(\frac{i}{\kappa}\nabla + \mathbf{A}_h^n \right) \Pi_h W_h \right\|_0 + \|\Pi_h W_h\|_0 \right).$$

Proof. Let $w_h = \Pi_h W_h$. It follows from (10) that

$$(43) \quad |(I_h L_{\mu_n}[\mathbf{A}^n]\psi, W_h)_{\mathcal{L}^2} - (L_{\mu_n}[\mathbf{A}^n]\psi, w_h)| \lesssim h \left\| \left(\frac{i}{\kappa}\nabla + \mathbf{A}^n \right)^2 \psi \right\|_1 \|w_h\|_0.$$

By the definition of $L_{\mu_n, h}[\mathbf{A}_h^n]$ in (15),

$$(L_{\mu_n, h}^n I_h\psi, W_h)_{\mathcal{L}^2} = - \left(\left(\frac{i}{\kappa}\nabla + \mathbf{A}_h^n \right) \Pi_L \psi, \left(\frac{i}{\kappa}\nabla + \mathbf{A}_h^n \right) w_h \right) - \mu_n (\Pi_L \psi, w_h).$$

It follows from the above equation and the integration by parts that

$$(44) \quad (L_{\mu_n, h}^n I_h\psi, W_h)_{\mathcal{L}^2} - (L_{\mu_n}[\mathbf{A}^n]\psi, w_h) = \sum_{i=1}^5 I_i,$$

where $I_1 = (\frac{i}{\kappa}\nabla(\psi - \Pi_L \psi), t_h)$, $I_2 = (\mathbf{A}^n(\psi - \Pi_L \psi), t_h)$, $I_3 = ((\mathbf{A}^n - \mathbf{A}_h^n)\Pi_L \psi, t_h)$, $I_4 = ((\frac{i}{\kappa}\nabla + \mathbf{A}^n)\psi, (\mathbf{A}^n - \mathbf{A}_h^n)w_h)$ and $I_5 = \mu_n((I - \Pi_L)\psi, w_h)$ with $t_h = (\frac{i}{\kappa}\nabla + \mathbf{A}_h^n)w_h$. It follows from the estimate (34) that

$$(45) \quad |I_1| + |I_2| + |I_3| + |I_4| + |I_5| \lesssim (\|e_{\mathbf{A}}^n\|_0 + h)\|t_h\|_0 + (\|e_{\mathbf{A}}^n\|_0 + h^2)\|w_h\|_0.$$

This, together with (43) and (44), leads to

$$\left| (\delta_n^1, W_h)_{\mathcal{L}^2} \right| \lesssim (\|e_{\mathbf{A}}^n\|_0 + h) \left(\left\| \left(\frac{i}{\kappa}\nabla + \mathbf{A}_h^n \right) w_h \right\|_0 + (\|e_{\mathbf{A}}^n\|_0 + h)\|w_h\|_0 \right),$$

which completes the proof. \square

Lemma 4. *Assume that Assumption 1 and 2 hold. Let $\mathbf{A}_h^0 = R_h \mathbf{A}^0$ and $\Psi_h^0 = I_h \psi^0$ with $\|\psi^0\|_\infty \leq 1$. The solution $\{(\mathbf{A}_h^n, \Psi_h^n)\}_{n=1}^{K_t}$ is generated by the discrete system (13) and (14) with the stabilizing parameter $\mu_n \geq \max\{\frac{C_2^2}{2C_1 C_3} + \frac{3}{8}\|\mathbf{A}_h^n\|_\infty^2, 2\}$ and time step $\tau_n = \tau$. For any $1 \leq n \leq K_t$,*

$$(46) \quad \|E_\psi^n\|_{\mathcal{L}^2}^2 + \tau \left\| \left(\frac{i}{\kappa}\nabla + \mathbf{A}_h^n \right) e_\psi^n \right\|_0^2 \leq (1 + C\tau)\|E_\psi^{n-1}\|_{\mathcal{L}^2}^2 + C\tau(\|e_{\mathbf{A}}^n\|_0^2 + \tau^2 + h^2).$$

Proof. It follows from (41) that

$$E_\psi^n = e^{\tau L_{\mu_n, h}^n} E_\psi^{n-1} + \int_0^\tau e^{(\tau-s)L_{\mu_n, h}^n} (\delta_n^1 + \delta_n^2 + \delta_n^3 + f_{\mu_n}(\Psi_h^{n-1}) - f_{\mu_n}(I_h\psi^{n-1})) ds.$$

Acting $I - \tau L_{\mu_n, h}^n$ on both sides of the equation above and taking ℓ^2 inner product with E_ψ^n yields

$$(47) \quad \begin{aligned} & \|E_\psi^n\|_{\ell^2}^2 + \tau \left\| \left(\frac{i}{\kappa} \nabla + \mathbf{A}_h^n \right) e_\psi^n \right\|_0^2 + \mu \tau \|E_\psi^n\|_{\ell^2}^2 \\ &= (q_1(\tau L_{\mu_n, h}^n) E_\psi^{n-1} + \tau q_2(\tau L_{\mu_n, h}^n) (f_{\mu_n}(\Psi_h^{n-1}) - f_{\mu_n}(I_h \psi^{n-1})), E_\psi^n)_{\ell^2} \\ & \quad + \int_0^\tau ((I - \tau L_{\mu_n, h}^n) e^{(\tau-s)L_{\mu_n, h}^n} \delta_n^1, E_\psi^n)_{\ell^2} ds + \int_0^\tau ((I - \tau L_{\mu_n, h}^n) e^{(\tau-s)L_{\mu_n, h}^n} (\delta_n^2 + \delta_n^3), E_\psi^n)_{\ell^2} ds, \end{aligned}$$

where $q_1(x) = (1-x)e^x$, $q_2(x) = \frac{(1-x)(e^x-1)}{x}$. Note that for any $x < 0$,

$$0 < q_1(x) < 1 < q_2(x) < 2.$$

Since $L_{\mu_n, h}^n$ is negative definite,

$$(48) \quad \begin{aligned} & |(q_1(\tau L_{\mu_n, h}^n) E_\psi^{n-1}, E_\psi^n)_{\ell^2}| \leq \|E_\psi^{n-1}\|_{\ell^2} \|E_\psi^n\|_{\ell^2}, \\ & |\tau q_2(\tau L_{\mu_n, h}^n) (f_{\mu_n}(U_h^{n-1}) - f_{\mu_n}(I_h \psi^{n-1})), E_\psi^n)_{\ell^2}| \leq C \tau \|E_\psi^{n-1}\|_{\ell^2} \|E_\psi^n\|_{\ell^2}. \end{aligned}$$

It follows from Lemma 3 that

$$|(I - \tau L_{\mu_n, h}^n) e^{(\tau-s)L_{\mu_n, h}^n} \delta_n^1, E_\psi^n)_{\ell^2}| \lesssim (\|e_{\mathbf{A}}^n\|_0 + h) \left(\left\| \left(\frac{i}{\kappa} \nabla + \mathbf{A}_h^n \right) t_h^n \right\|_0 + \|t_h^n\|_0 \right),$$

where $t_h^n = (I - \tau L_{\mu_n, h}^n)^T e^{(\tau-s)L_{\mu_n, h}^n} E_\psi^n$. Since $0 < q_1(x) < 1$,

$$(49) \quad \left| \int_0^\tau ((I - \tau L_{\mu_n, h}^n) e^{(\tau-s)L_{\mu_n, h}^n} \delta_n^1, E_\psi^n)_{\ell^2} ds \right| \lesssim \tau (\|e_{\mathbf{A}}^n\|_0 + h) \left(\left\| \left(\frac{i}{\kappa} \nabla + \mathbf{A}_h^n \right) e_\psi^n \right\|_0 + \|E_\psi^n\|_{\ell^2} \right).$$

Note that $\|\delta_n^2\|_0 + \|\delta_n^3\|_0 \lesssim \tau$. Thus,

$$(50) \quad \left| \int_0^\tau ((I - \tau L_{\mu_n, h}^n) e^{(\tau-s)L_{\mu_n, h}^n} (\delta_n^2 + \delta_n^3), E_\psi^n)_{\ell^2} ds \right| \lesssim \tau^2 \|E_\psi^n\|_{\ell^2}.$$

A substitution of (48), (49) and (50) into (47) gives

$$\begin{aligned} & \|E_\psi^n\|_{\ell^2}^2 + \tau \left\| \left(\frac{i}{\kappa} \nabla + \mathbf{A}_h^n \right) e_\psi^n \right\|_0^2 + \frac{\mu_n \tau}{2} \|E_\psi^{n-1}\|_{\ell^2}^2 \\ & \leq (1 + C\tau) \|E_\psi^{n-1}\|_{\ell^2} \|E_\psi^n\|_{\ell^2} + C\tau (\|e_{\mathbf{A}}^n\|_0 + h) \left\| \left(\frac{i}{\kappa} \nabla + \mathbf{A}_h^n \right) e_\psi^n \right\|_0 + C\tau \|E_\psi^n\|_0 (\|e_{\mathbf{A}}^n\|_{\ell^2} + \|E_\psi^n\|_{\ell^2} + \tau + h). \end{aligned}$$

By the Young's inequality,

$$\|E_\psi^n\|_{\ell^2}^2 + \tau \left\| \left(\frac{i}{\kappa} \nabla + \mathbf{A}_h^n \right) e_\psi^n \right\|_0^2 \leq (1 + C\tau) \|E_\psi^{n-1}\|_{\ell^2}^2 + C\tau (\|e_{\mathbf{A}}^n\|_0^2 + \tau^2 + h^2),$$

which completes the proof. \square

The following theorem presents the main result of the error estimate of the proposed numerical scheme.

Theorem 3. *Assume that Assumption 1 and 2 hold. Let $\mathbf{A}_h^0 = R_h \mathbf{A}^0$ and $\Psi_h^0 = I_h \psi^0$ with $\|\psi_0\|_\infty \leq 1$. The solution $\{(\mathbf{A}_h^n, \Psi_h^n)\}_{n=1}^{K_t}$ is generated by the discrete system (13) and (14) with the stabilizing parameter $\mu_n \geq \max\{(\frac{C_2^2}{2C_1C_3} + \frac{3}{8}) \|\mathbf{A}_h^n\|_\infty^2, 2\}$ and time step $\tau_n = \tau$. For any $1 \leq n \leq K_t$,*

$$\|\mathbf{A}_h^n - \mathbf{A}^n\|_0 + \|\nabla \times (\mathbf{A}_h^n - \mathbf{A}^n)\|_0 + \|\psi_h^n - \psi^n\|_0 \lesssim \tau + h.$$

Proof. Denote $T^n = \|E_\psi^n\|_{\ell^2}^2 + \sigma \|e_{\mathbf{A}}^n\|^2 + \tau \left\| \left(\frac{i}{\kappa} \nabla + \mathbf{A}_h^n \right) e_\psi^n \right\|_0^2 + 2\tau \|\nabla \times e_{\mathbf{A}}^n\|_0^2$. By the estimates (35) and (46), $T^n \leq (1 + C\tau) T^{n-1} + C\tau (h^2 + \tau^2)$, which implies that $T^n \leq (1 + C\tau)^n T^0 + C\tau (\tau^2 + h^2) \sum_{i=1}^n (1 + C\tau)^i$. Note that there exists constant C_0 such that $|(1 + C\tau)^n| + |\tau \sum_{i=1}^n (1 + C\tau)^i| \leq C_0$. This, together with the fact that $|T^0| \lesssim h^2$, leads to

$$(51) \quad \|e_{\mathbf{A}}^n\|_0 + \|E_\psi^n\|_{\ell^2} \lesssim \tau + h.$$

As a consequence, the estimate (46) reads $\|E_\psi^n\|_{\ell^2}^2 + \tau\|(\frac{i}{\kappa}\nabla + \mathbf{A}_h^n)e_\psi^n\|_0^2 \leq (1 + C\tau)\|E_\psi^{n-1}\|_{\ell^2}^2 + C\tau(\tau^2 + h^2)$, which leads to

$$\|E_\psi^n\|_{\ell^2}^2 + \tau \sum_{j=1}^n \|(\frac{i}{\kappa}\nabla + \mathbf{A}_h^j)e_\psi^j\|_0^2 \leq (1 + C\tau)^n \|E_\psi^0\|_{\ell^2}^2 + C\tau(\tau^2 + h^2) \sum_{j=0}^{n-1} (1 + C\tau)^j \leq C(\tau^2 + h^2).$$

Substituting this into the estimate (36) yields

$$\|\nabla \times e_{\mathbf{A}}^n\|_0^2 \leq \|\nabla \times e_{\mathbf{A}}^0\|_0^2 + C\tau \sum_{j=0}^{n-1} \|(\frac{i}{\kappa}\nabla + \mathbf{A}_h^j)e_\psi^j\|_0^2 + C(\tau^2 + h^2) \leq C(\tau^2 + h^2).$$

A combination of the estimate above and (51) gives $\|e_{\mathbf{A}}^n\|_0 + \|E_\psi^n\|_{\ell^2} + \|\nabla \times e_{\mathbf{A}}^n\|_0 \lesssim \tau + h$. This, together with the estimates (12) and (34), completes the proof. \square

Remark 2. In the decoupled system (13) and (14), the first order convergence rate of $\|\mathbf{A}_h^n - \mathbf{A}^n\|_0$ is one degree lower than that of the projection error $\|R_h \mathbf{A}^n - \mathbf{A}^n\|_0$. The gap is caused by nonlinearity, that is the explicit gradient term $g(\psi_h^{n-1})$ in (13). We can fix the gap by applying the gradient recovery technique in [32] and replace $g(\psi_h^{n-1})$ in (13) by the recovered gradient, that is to seek $(\hat{\mathbf{A}}_h^n, \hat{\psi}_h^n)$ such that

$$(d_t^n \hat{\mathbf{A}}_h, \mathbf{B}_h) + D(\hat{\psi}_h^{n-1}; \hat{\mathbf{A}}_h^n, \mathbf{B}_h) = (\mathbf{H}^n, \nabla \times \mathbf{B}_h) - (g_M(\hat{\psi}_h^{n-1}, \hat{\psi}_h^{n-1}), \mathbf{B}_h),$$

for any $\mathbf{B}_h \in Q_h$ and $\hat{\Psi}_h^n = \hat{U}_h(t_n)$ satisfying (14) with $\hat{\Psi}_h^0 = I_h \psi^0$ and $\hat{\mathbf{A}}_h^0 = R_h \mathbf{A}^0$, where $g_M(\psi_h, \psi_h) = \frac{i}{2\kappa}(\psi_h^*(K_h \psi_h) - \psi_h(K_h \psi_h^*))$ with recovered gradient $K_h \psi_h$.

5. NUMERICAL EXAMPLES

In this section, we present some numerical examples to verify the theoretical result and show the vortex motions of superconductors in an external magnetic field.

5.1. Example 1. Consider the artificial example on $\Omega = (0, 1)^2$ with $\kappa = 1$

$$(52) \quad \begin{cases} \partial_t \psi = -\left(\frac{i}{\kappa}\nabla + \mathbf{A}\right)^2 \psi + \psi - |\psi|^2 \psi + g & \text{in } \Omega, \\ \partial_t \mathbf{A} = \frac{1}{2i\kappa}(\psi^* \nabla \psi - \psi \nabla \psi^*) - |\psi|^2 \mathbf{A} - \nabla \times \nabla \times \mathbf{A} + f & \text{in } \Omega, \end{cases}$$

and the boundary and initial conditions (2). The functions f , g , ψ^0 and \mathbf{A}^0 are chosen corresponding to the exact solution $\psi = e^{-t}(\cos(2\pi x) + i \cos(\pi y))$, $\mathbf{A} = [e^{t-y} \sin(\pi x), e^{t-x} \sin(2\pi y)]^T$ with $\mathbf{H} = -e^{t-x} \sin(2\pi y) + e^{t-y} \sin(\pi x)$. We set the terminal time $T = 1$ in this example. Table 1 records the L^2 -norm error of \mathbf{A}_h , $\nabla \times \mathbf{A}_h$, ψ_h and $\nabla \psi_h$ on uniform triangulations with mesh size h , which coincide with the convergence result in Theorem 3 and shows the accuracy of the proposed numerical scheme when the solution is smooth enough.

1/h	$\ \mathbf{A} - \mathbf{A}_h\ _0$	rate	$\ \nabla \times (\mathbf{A} - \mathbf{A}_h)\ _0$	rate	$\ \psi - \psi_h\ _0$	rate	$\ \nabla(\psi - \psi_h)\ _0$	rate
8	2.97E-01	1.33	3.23E-01	0.53	4.22E-01	3.10	5.50E-01	2.08
16	1.47E-01	1.01	1.64E-01	0.97	1.26E-01	1.74	2.31E-01	1.25
32	7.08E-02	1.05	8.26E-02	0.99	3.63E-02	1.79	1.09E-01	1.09
64	3.48E-02	1.02	4.13E-02	1.00	1.21E-02	1.59	5.32E-02	1.03
128	1.73E-02	1.01	2.07E-02	1.00	4.86E-03	1.31	2.64E-02	1.01
256	8.62E-03	1.00	1.03E-02	1.00	2.23E-03	1.12	1.32E-02	1.00
512	4.31E-03	1.00	5.17E-03	1.00	1.08E-03	1.04	6.59E-03	1.00

TABLE 1. The relative errors with time step $\tau = h$.

5.2. Example 2: L-shaped superconductor. We use the proposed formulation to simulate the vortex dynamics in the superconductor $\Omega = (-0.5, 0.5)^2 \setminus [0, 0.5] \times [-0.5, 0]$ with the Ginzburg-Landau parameter $\kappa = 10$. The initial conditions and applied magnetic field are $\psi^0 = 0.6 + 0.8i$, $\mathbf{A}^0 = (0, 0)$ and $\mathbf{H} = 5$. This example was tested before by different methods, see [11, 24] for reference. We simulate the problem on a uniform triangulation with $M = 16$ nodes per unit length on each side and the stabilization parameter $\mu_h = 2$. Since the discrete energy decays as proved in Theorem 1, we adopt the adaptive time stepping scheme in [30] which takes the form $\tau^n = \max\{\tau_{\min}, \frac{\tau_{\max}}{\sqrt{1 + \alpha \frac{C_h^{n-1} - C_h^{n-2}}{\tau^{n-1}}}}\}$, where the

positive constant $\alpha = 10^5$, $\tau_{\max} = 0.2$ and $\tau_{\min} = 0.02$. Fig.1 plots the discrete energy of the proposed scheme and the time step for $t \leq 20$, which verifies the theoretical result in Theorem 1. In this example, the time steps are almost $\tau_{\max} = 0.2$ when $t > 5$ due to the slow change in energy. Compared to the schemes in [11, 24] with fixed time steps, the new scheme with adaptive time stepping saves large amount of computational time, especially in long time simulations.

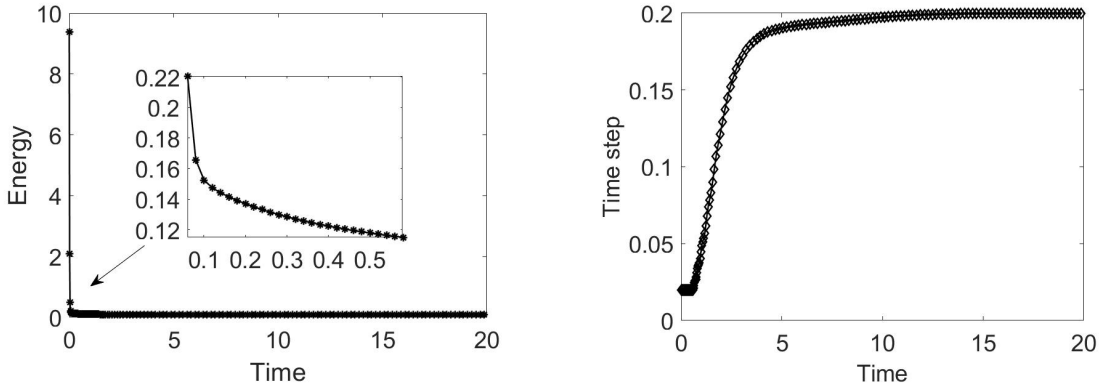


FIGURE 1. Discrete energy and time steps for Example 2.

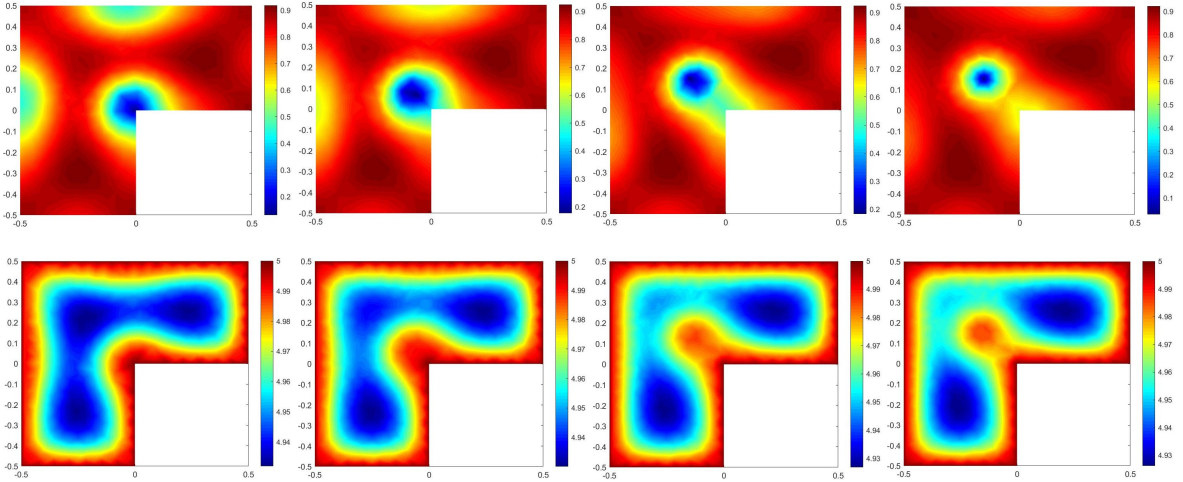


FIGURE 2. $|\psi_h|$ (above) and $\nabla \times \mathbf{A}_h$ (below) at $T = 5, 10, 20$ and 40 for Example 2.

Fig. 2 plots $|\psi_h|$ and $\nabla \times \mathbf{A}_h$ by the scheme (13) and (14). It shows that one vortex enters the material from the re-entrant corner as the time increases, which is similar to those reported in [11, 24].

Physically speaking, the superconducting density should be between 0 and 1, and the average magnetic field should be less than H when the superconductor is in a mixed state [8]. The numerical results in Fig.2 indicates that the magnitude of ψ_h by the proposed scheme is indeed bounded by 1, and the magnetic field $\nabla \times \mathbf{A}_h$ is also bounded by H , which coincide with physical observation. It is reported in [11, 24] that the conventional finite element method for solving the Ginzburg-Landau equations under temporal gauge is unstable with respect to the mesh size. To be specific, this conventional method with $M = 16$ and 32 gives a nonphysical simulation when $T = 40$, but the one with $M = 64$ exhibits the correct phenomenon. The numerical solution of the proposed approach in Fig.2 implies that the new approach is stable and correct even on a relative coarse triangulation with $M = 16$. The reason why the proposed approach works while the conventional one does not is that the true solution \mathbf{A} of this problem is not in H^1 space any more, which leads to an approximation to a projection of \mathbf{A} , not an approximation to \mathbf{A} . The proposed scheme solves \mathbf{A} in $H(\text{curl})$ space with no additional boundary condition, and gives a stable vortex dynamics.

5.3. Example 3: Hollow superconductor. We present simulations of vortex dynamics of a type II superconductor in a square domain $[0, 10]^2$ with four square holes $\{(x, y) : x \text{ and } y \in [2, 3] \cup [7, 8]\}$. We set $\sigma = 1$, $\kappa = 4$, $\psi^0 = 1.0$, $\mathbf{A}^0 = (0, 0)$, and test on two different external magnetic fields $H = 1.1$ and 1.9. The example was tested before in [15, 29]. We simulate the motion on a triangulation generated by Gmsh with 403246 and 786482 elements for the case $H = 1.1$ and $H = 1.9$, respectively. We take the same adaptive time stepping strategy as in Example 2.

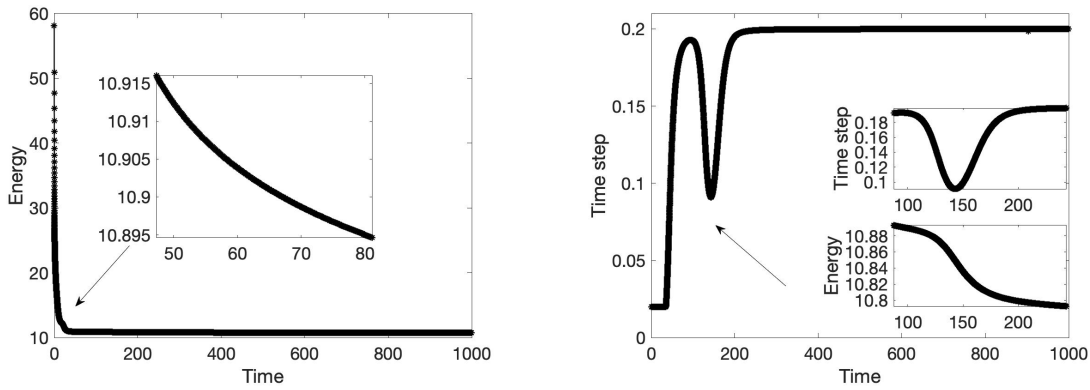


FIGURE 3. Discrete energy and time steps for Example 3 with $H = 1.1$.

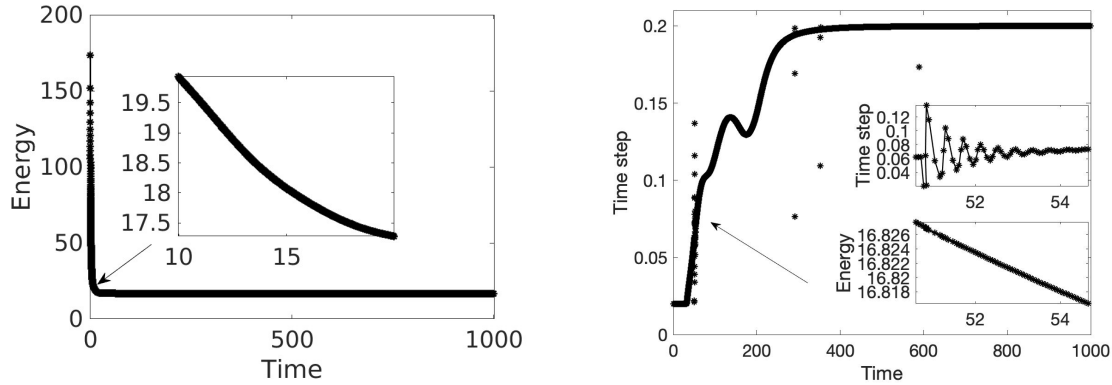


FIGURE 4. Discrete energy and time steps for Example 3 with $H = 1.9$.

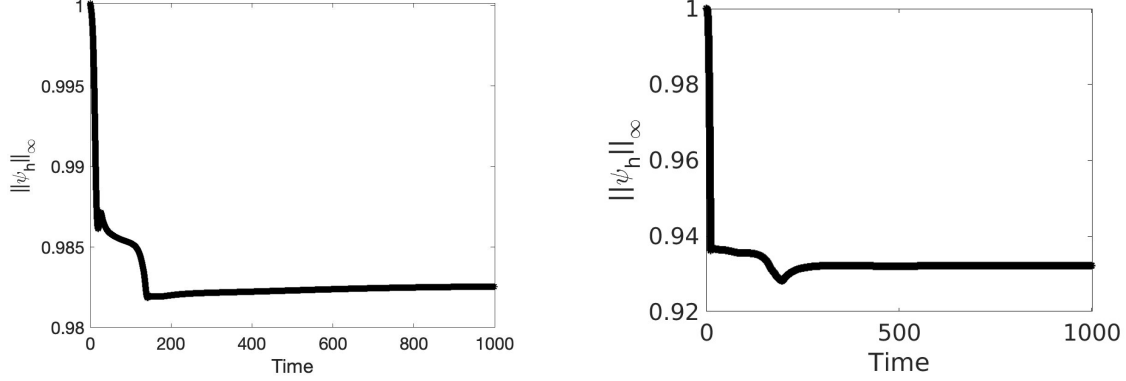


FIGURE 5. Discrete maximum bound of $|\psi|$ for Example 3 with $H = 1.1$ (left) and $H = 1.9$ (right).

Fig.3 and Fig.4 plot the discrete energy and the time steps of the proposed scheme with $H = 1.1$ and $H = 1.9$ when $t \leq 1000$, respectively. As shown in Fig.3, the adaptive time stepping can successfully capture the change of discrete energy and save the computational time. Note that the time steps are nearly $\tau_{\max} = 0.2$ when $t \geq 100$ for $H = 1.1$ and when $t \geq 400$ for $H = 1.9$, which is much larger than those employed in [?, 21]. This implies that the new scheme with adaptive time stepping is much more efficient in long time simulations. As shown in Fig.4, the discrete energy decays even when the time step is not changing continuously which also verifies the unconditional energy decay property of the proposed numerical scheme.

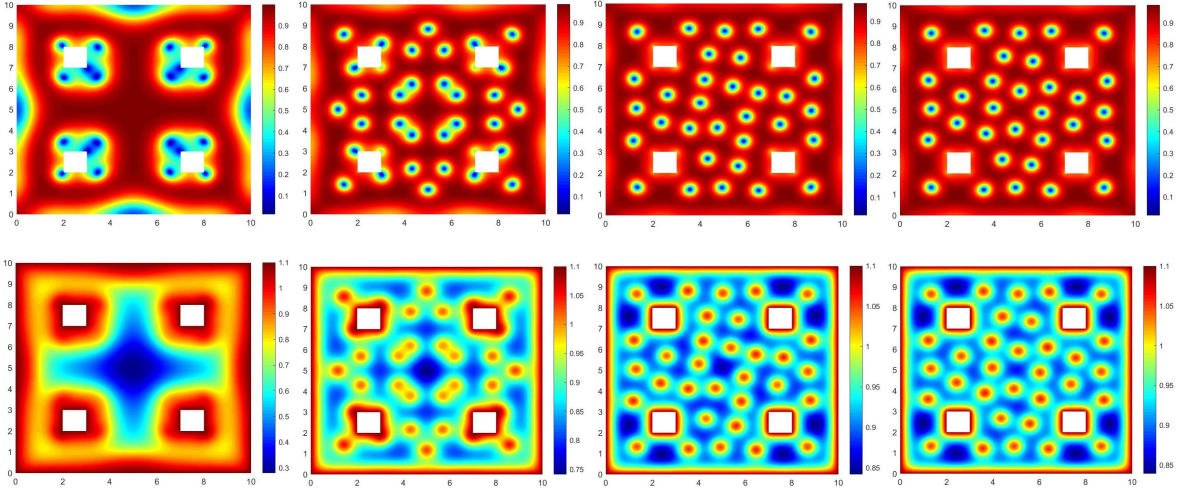


FIGURE 6. $|\psi_h|$ (above) and $\nabla \times A_h$ (below) at $T = 10, 50, 200, 500$ for Example 3 with $H = 1.1$ on triangulation with 516526 elements.

Fig.6 and Fig.7 plot $|\psi_h|$ and $\nabla \times A_h$ at $T = 10, 50, 200$ and 500 for $H = 1.1$ and $H = 1.9$, respectively. As observed in Fig.6 and Fig.7, the vortices start to penetrate the material near the four square holes. When H becomes larger, more vortices are generated and triangulation with much smaller mesh size is required to resolve the singularity of solutions, which coincides with the physical phenomenon. Physically speaking, the penetrated magnetic flux will separate into the smallest bundle to guarantee the largest interface area since the interface energy in type-II superconductors is negative,

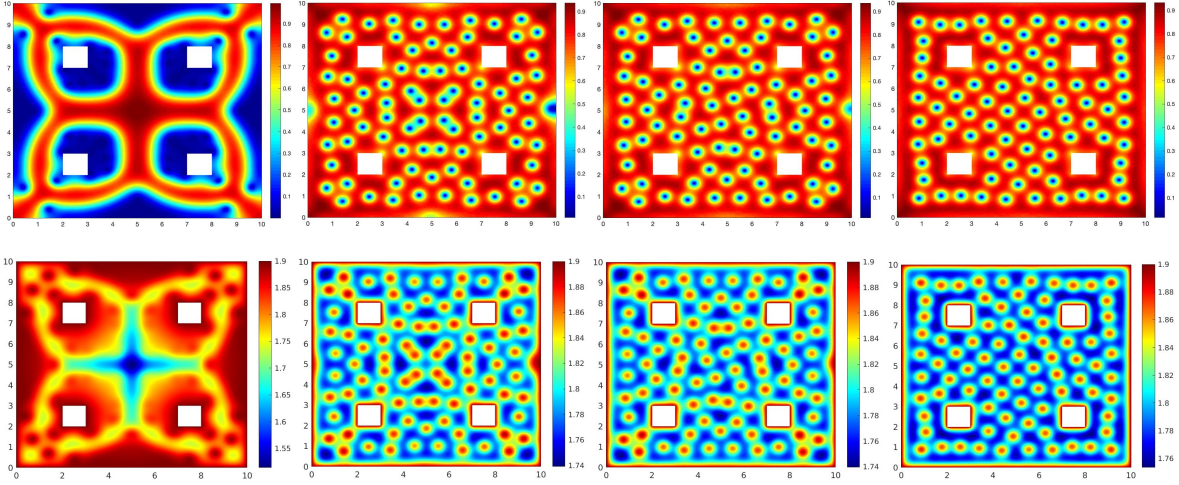


FIGURE 7. $|\psi_h|$ (above) and $\nabla \times A_h$ (below) at $T = 10, 50, 200, 500$ for Example 3 with $H = 1.9$.

and the vortices form a lattice because of the weak repulsive interactions among them. In long-time simulations, discrete schemes with high convergence result may produce some nonphysical numerical phenomenon because of the lack of stability. This nonphysical phenomenon often happens near the reentrant corners when the applied magnetic field is strong. The vortex dynamics in Fig.6 and Fig.7 shows that the proposed numerical scheme is robust and stable even when $H = 1.9$.

6. CONCLUSIONS

In this paper, we propose a decoupled scheme for the TDGL equations under temporal gauge by combining the ETD method and the backward Euler method for time discretization and finite element methods for spatial discretization. Compared to the existing schemes for the TDGL equations, the proposed numerical scheme admits three advantages. Firstly, the scheme and all the energy stability analysis, MBP analysis and error analysis work for superconductors with complicate shapes. Secondly an unconditional energy dissipation law is proved for the proposed scheme. This allows the application of adaptive time stepping algorithms which can significantly speed up simulations compared to other numerical schemes for the TDGL equations in the literature using fixed time step. Thirdly, the discrete MBP is proved for the numerical order parameter which indicates the stability of the numerical scheme, while no other numerical schemes using finite element methods can preserve the MBP property theoretically. The analyzing technique can also be used in other problems with complex order parameter. Last, the relatively low regularity of the numerical solutions prevents the appearance of some nonphysical numerical solutions. For the discrete scheme in Remark 2 with gradient recovery techniques, the discrete MBP is also guaranteed under the mesh requirements in Assumption 1. But how to preserve the energy dissipation law in discrete sense is still an open problem. A major difficulty comes from the discretization of the coupling nonlinear term in the equations for both magnetic field and order parameter. The solutions of the proposed scheme converge at the rate one with respect to time step. How to design a MBP preserving numerical scheme with a higher accuracy in time is also open which requires some delicate treatment with respect to the coupling terms of the TDGL equations. Fast solver of numerical schemes is important in simulating the vortex motion of superconductors, especially when the shape of the superconductor is not smooth and a strong external magnetic field is applied. The design of fast solvers for the proposed numerical scheme and the theoretical analysis to guarantee the efficiency of the solver deserve deeper study.

REFERENCES

- [1] Gregory Beylkin, James M Keiser, and Lev Vozovoi. A new class of time discretization schemes for the solution of nonlinear pdes. *Journal of computational physics*, 147(2):362–387, 1998.
- [2] S Jonathan Chapman, Sam D Howison, and John R Ockendon. Macroscopic models for superconductivity. *SIAM Review*, 34(4):529–560, 1992.
- [3] Zhiming Chen. Mixed finite element methods for a dynamical Ginzburg–Landau model in superconductivity. *Numerische Mathematik*, 76(3):323–353, 1997.
- [4] Zhiming Chen, K-H Hoffmann, and Jin Liang. On a non-stationary Ginzburg–Landau superconductivity model. *Mathematical Methods in the Applied Sciences*, 16(12):855–875, 1993.
- [5] Steven M Cox and Paul C Matthews. Exponential time differencing for stiff systems. *Journal of Computational Physics*, 176(2):430–455, 2002.
- [6] Qiang Du. Finite element methods for the time-dependent Ginzburg–Landau model of superconductivity. *Computers & Mathematics with Applications*, 27(12):119–133, 1994.
- [7] Qiang Du. Discrete gauge invariant approximations of a time dependent Ginzburg–Landau model of superconductivity. *Mathematics of computation*, 67(223):965–986, 1998.
- [8] Qiang Du, Max D Gunzburger, and Janet S Peterson. Analysis and approximation of the Ginzburg–Landau model of superconductivity. *SIAM Review*, 34(1):54–81, 1992.
- [9] Qiang Du, Lili Ju, Xiao Li, and Zhonghua Qiao. Maximum principle preserving exponential time differencing schemes for the nonlocal Allen–Cahn equation. *SIAM Journal on numerical analysis*, 57(2):875–898, 2019.
- [10] Qiang Du, Lili Ju, Xiao Li, and Zhonghua Qiao. Maximum bound principles for a class of semilinear parabolic equations and exponential time-differencing schemes. *SIAM Review*, 63(2):317–359, 2021.
- [11] Huadong Gao. Efficient numerical solution of dynamical Ginzburg–Landau equations under the lorentz gauge. *Communications in Computational Physics*, 22(1):182–201, 2017.
- [12] Huadong Gao, Lili Ju, and Wen Xie. A stabilized semi-implicit euler gauge-invariant method for the time-dependent Ginzburg–Landau equations. *Journal of Scientific Computing*, 80(2):1083–1115, 2019.
- [13] Huadong Gao, Buyang Li, and Weiwei Sun. Optimal error estimates of linearized Crank–Nicolson Galerkin FEMs for the time-dependent Ginzburg–Landau equations in superconductivity. *SIAM Journal on Numerical Analysis*, 52(3):1183–1202, 2014.
- [14] Huadong Gao and Weiwei Sun. An efficient fully linearized semi-implicit Galerkin-mixed FEM for the dynamical Ginzburg–Landau equations of superconductivity. *Journal of Computational Physics*, 294:329–345, 2015.
- [15] Huadong Gao and Weiwei Sun. A new mixed formulation and efficient numerical solution of Ginzburg–Landau equations under the temporal gauge. *SIAM Journal on Scientific Computing*, 38(3):A1339–A1357, 2016.
- [16] Huadong Gao and Weiwei Sun. Analysis of linearized Galerkin-mixed FEMs for the time-dependent Ginzburg–Landau equations of superconductivity. *Advances in Computational Mathematics*, 44(3):923–949, 2018.
- [17] V Ginzburg and L Landau. Theory of superconductivity. *Zh.Eksp.Teor.Fiz*, 20:1064–1082, 1950.
- [18] Lev Petrovich GOR’KOV and GM Eliashberg. Generalization of the Ginzburg–Landau equations for non-stationary problems in the case of alloys with paramagnetic impurities. *Journal of Experimental and Theoretical Physics*, 27:328–334, 1968.
- [19] Marlis Hochbruck and Alexander Ostermann. Explicit exponential runge–kutta methods for semilinear parabolic problems. *SIAM Journal on Numerical Analysis*, 43(3):1069–1090, 2005.
- [20] Marlis Hochbruck and Alexander Ostermann. Exponential integrators. *Acta Numerica*, 19:209–286, 2010.
- [21] Qingguo Hong, Limin Ma, and Jinchao Xu. An efficient iterative method for dynamical Ginzburg–Landau equations. *arXiv:2207.01425*, 2022.
- [22] Buyang Li, Kai Wang, and Zhimin Zhang. A hodge decomposition method for dynamic Ginzburg–Landau equations in nonsmooth domains—a second approach. *Communications in Computational Physics*, 28(2):768–802, 2020.
- [23] Buyang Li and Zhimin Zhang. A new approach for numerical simulation of the time-dependent Ginzburg–Landau equations. *Journal of Computational Physics*, 303:238–250, 2015.
- [24] Buyang Li and Zhimin Zhang. A new approach for numerical simulation of the time-dependent Ginzburg–Landau equations. *Journal of Computational Physics*, 303:238–250, 2015.
- [25] Buyang Li and Zhimin Zhang. Mathematical and numerical analysis of the time-dependent Ginzburg–Landau equations in nonconvex polygons based on hodge decomposition. *Mathematics of Computation*, 86(306):1579–1608, 2017.
- [26] Mo Mu. A linearized Crank–Nicolson-Galerkin method for the Ginzburg–Landau model. *SIAM Journal on Scientific Computing*, 18(4):1028–1039, 1997.
- [27] Mo Mu and Yunqing Huang. An alternating Crank–Nicolson method for decoupling the Ginzburg–Landau equations. *SIAM journal on numerical analysis*, 35(5):1740–1761, 1998.
- [28] Jitse Niesen and Will M Wright. A Krylov subspace algorithm for evaluating the ϕ -functions appearing in exponential integrators. *ACM Transactions on Mathematical Software*, 38(3):1–19, 2012.
- [29] Lin Peng, Zejiang Wei, and Danhua Xu. Vortex states in mesoscopic superconductors with a complex geometry: A finite element analysis. *International Journal of Modern Physics B*, 28(20):1450127, 2014.
- [30] Zhonghua Qiao, Zhengru Zhang, and Tao Tang. An adaptive time-stepping strategy for the molecular beam epitaxy models. *SIAM Journal on Scientific Computing*, 33(3):1395–1414, 2011.

- [31] Michael Tinkham. *Introduction to superconductivity*. Courier Corporation, 2004.
- [32] Zhimin Zhang and Ahmed Naga. A new finite element gradient recovery method: superconvergence property. *SIAM Journal on Scientific Computing*, 26(4):1192–1213, 2005.

SCHOOL OF MATHEMATICS AND STATISTICS, WUHAN UNIVERSITY, HUBEI, PRC. LIMIN18@WHU.EDU.CN

DEPARTMENT OF APPLIED MATHEMATICS, THE HONG KONG POLYTECHNIC UNIVERSITY, HUNG HOM, HONG KONG. ZHONGHUA.QIAO@POLYU.EDU.HK